I.FAST

Innovation Fostering in Accelerator Science and Technology

Horizon 2020 Research Infrastructures GA n° 101004730

MILESTONE REPORT

Target manufacturing and characterization

MILESTONE: MS23

Document identifier:	IFAST_MS23
Due date of milestone:	End of Month 12 (April 2022)
Report release date:	02/08/2022
Work package:	WP6: [Novel particle accelerators concepts and technologies]
Lead beneficiary:	CNRS
Document status:	Final

ABSTRACT

Laser-Plasma Accelerators (LPA) exploits electric fields exceeding 100 GV/m to produce ultrashort electron bunches. These unique features open up new prospects for ultrafast-physics and the development of compact accelerators, for instance. Yet, LPAs suffer from an inferior beam quality and stability. One of the reasons for these weaknesses is a poor control of the target properties. Task 6.3 aims at developing and test targets of superior quality for extending the beam energy and improving its reliability. Here we report on Milestone MS23 which comprises the target manufacturing and characterisation.

For more information on I.FAST, its partners and contributors please see https://ifast-project.eu/

This project has received funding from the European Union's Horizon 2020 Research and Innovation programme under Grant Agreement No 101004730. I.FAST began in May 2021 and will run for 4 years.

Delivery Slip

	Name	Partner	Date
Authored by	Dr. Vidmantas Tomkus, Dr. Gediminas Račiukaitis	FTMC	22/04/2022
Edited by	C. Thaury	CNRS	28/04/2022
Reviewed by	M. Vretenar on behalf of the Steering Committee	CERN	02/08/2022
Approved by	Steering Committee		02/08/2022

TABLE OF CONTENTS

1. Introduction

The objective of work package 6.3 is to develop multi-scale innovative targets for laser-plasma accelerators (LWFA) and demonstrate improved electron beam features with the new targets. This objective is planned to be achieved using better control of the plasma target properties. Targets are manufactured from fused silica using an innovative hybrid 3D laser machining technique to ensure better control of the plasma density on the < 100 µm scale with respect to conventional machining techniques such as electro-erosion. The Milestone MS23 comprises the target manufacturing and characterisation. Afterwards, the targets will be tested and optimised at laser-plasma acceleration facilities of CNRS/LOA.

2. Methods of 3D Laser manufacturing of nozzles

To manufacture nozzles, a hybrid 3D laser machining technique was implemented [1]. Fast removal by nanosecond rear-side processing was used for the frame manufacturing from fused silica. Gas jet nozzles were fabricated using the second harmonics (532 nm) of a diode-pumped solid-state (DPSS) laser (from Ekspla). The pulse duration, measured at full-width at half-maximum, was 4.5 ns. The laser system provided the maximum average laser power of 18 W at a 200 kHz pulse repetition rate. The diameter of the focused beam at the $1/e^2$ level equalled to 10.5 µm. Typical pulse energy and laser fluence were 90 µJ and 210 J/cm^2, respectively. The material removal rate was over 2 mm^3/s. The surface roughness of 5-8 µm of the nozzle walls and edge chipping of the nozzle outlet limited the possibility of manufacturing channels less than 200 – 300 µm. Femtosecond Laser-assisted Selective Chemical Etching (FLSE) technique was implemented for the high-precision channel formation. For the channel modification, a femtosecond laser system (Yb: ”KGW Pharos” laser from Light Conversion) wavelength of 515 nm, pulse duration FWHM of 300 fs, and pulse energy <1 µJ was used. The repetition rate was set to 500 kHz, and the processing speed was 0.5 mm/s to ensure a 1000 pulses/µm density. The laser beam was focused with a 100x microscope objective (from Mitutoyo, NA=0.5) to achieve a ~2 µm spot size. The total laser fabrication time of the 100 µm diameter channel was ~21 min. Then, the laser-modified areas (microchannels) were etched in a KOH solution of 10M concentration for 22 hours. The pre-compensation of the modified area has improved the diameter accuracy control up to +/- 2 µm. The formation of nozzles using the FLSE technique enabled the formation of nozzles with dimensions of less than 40 µm and surface roughness R_{zd} < 0.7 µm. However, because of the long fabrication time, this technique was not suitable for high-volume processing. The implementation of a hybrid 3D laser machining technique using the advantages of nanosecond fast removal of the material and high accuracy of FLICE processing is optimal for the manufacturing of micronozzles from fused silica. In addition, the fused silica nozzles have a higher damage threshold than metallic ones, leading to a higher resistance to laser radiation and reliability in operation.

3. Micrometric Supersonic nozzles for laser-plasma interaction

For the operation with kHz class 1 TW laser, micrometric supersonic nozzles with 40 - 60 µm throat and 120 – 180 µm exit diameter were manufactured (Fig.1). The 3.8 mJ energy of such a laser-focused by an f/4 off-axis parabola into the 6.2 µm × 5.5 µm FWHM focal spot corresponds to a Rayleigh range of $Z_R \sim 100$ µm. The 4 fs laser pulses yield an intensity of $I = 2.0 \times 10^{18}$ W cm^{-2} and a normalised vector potential $a_0 \simeq 1.0$. For the efficient laser wakefield acceleration, plasma targets with a length of ~ 100 µm and plasma concentration of 5×10^{19} cm^{-3} - 1×10^{20} cm^{-3} are required [2].

In Fig. 1, the pictures of micrometric supersonic nozzles manufactured using the FLICE technique are shown. To increase the formation precision, the initial pre-compensation of the channel diameter was implemented. Some of the manufactured nozzles had problems with residual stresses of the material, leading to crack formation in fused silica (Fig.1d). Annealing of the material and careful

selection of irradiation regime allowed to reach the required parameters without cracking. In Fig. 1b-d, the tomography slices of the nozzle of the 60 μm throat and 180 μm exit diameter are presented [3].

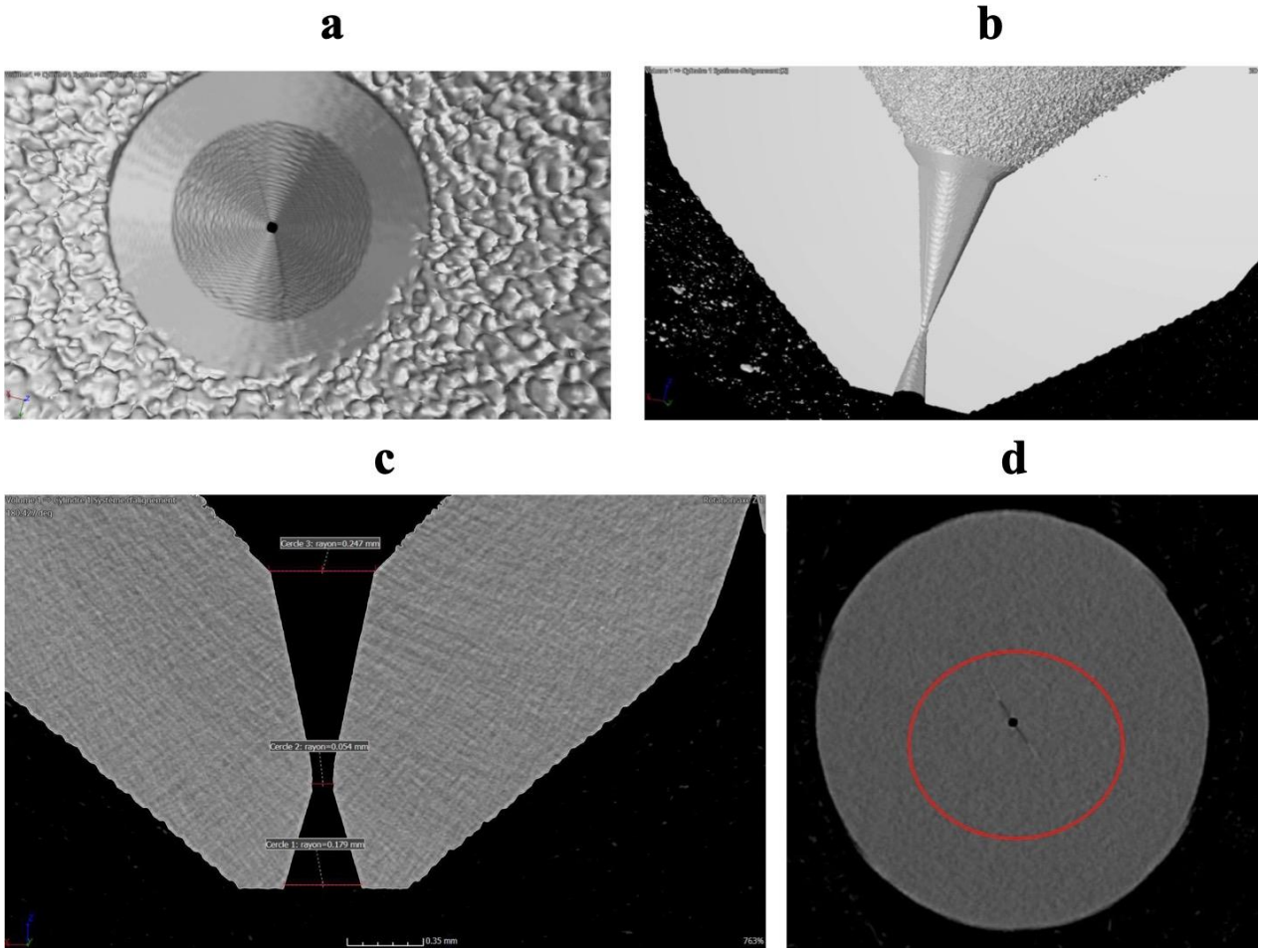

Figure 1: *The top view (a) and tomography slices of a supersonic micronozzle with a diameter of 60/180 μm (b-d). The cracks in fused silica are caused by residual stresses in the material after the modification with an excessive accumulated density of the femtosecond laser pulses (d).*

The gas and plasma profiles were characterised using a quadriwave lateral shearing interferometer [4], and the density maps were obtained via Abel inversion of the measured phase maps. In Fig.2, the reconstructed distributions of N_2 nitrogen gas, at backing pressure of 15 bar (Fig.2a) and 20 bar (Fig.2d) are shown. For a nitrogen gas, the pre-pulse of the laser ionises the molecular and L-shell atomic bonds of N_2, thus releasing 10 electrons per molecule. For backing pressures between 12 bar and 100 bar, a peak electron density from 4.2×10^{19} cm^{-3} to 3.5×10^{20} cm^{-3} at 150 μm above the

nozzle can be reached. Using this type of nozzles and kHz class 1 TW laser, the electrons can be accelerated up to the energies of 2-3 MeV.

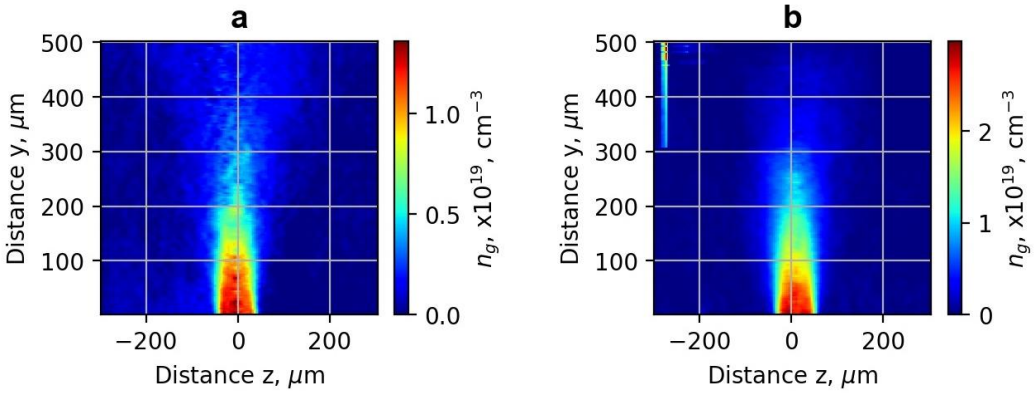

Figure 2: *Reconstructed distribution of N2 gas concentration of the nozzle with 60 μm throat and 180 μm exit diameter at 15 bar (a) and 20 bar (b) of backing pressure.*

4. Symmetric shocked micronozzles

The plasma downward density injection scheme has been used in numerous experiments on laser wakefield acceleration, and it increases the electron beam quality and stability. The plasma wavelength increases abruptly because of the sudden change in plasma density, and background electrons are trapped by the plasma wake. Shocks in supersonic flows produce a downward density transition of plasma concentration followed by a plateau needed for the injection scheme [5]. In Fig. 3a, a nozzle configuration is shown, where a straight duct is added at the end of the diverging section of a “de Laval” nozzle. It induces a shock-front of angle $\beta - \theta$ with the longitudinal axis. The distribution of gas density was simulated using ANSYS Fluent software. The shock fronts then converge on-axis at a distance z_m from the nozzle exit determined by the shock angle and the length of the straight duct. In Fig. 3b,c, the results of the measurement performed on a jet with $\varphi_t = 60$ μm, $\varphi_e = 180$ μm, and a 10^o diverging section, with a straight duct length L = 100μm, and the comparison with the simulated profile are presented.

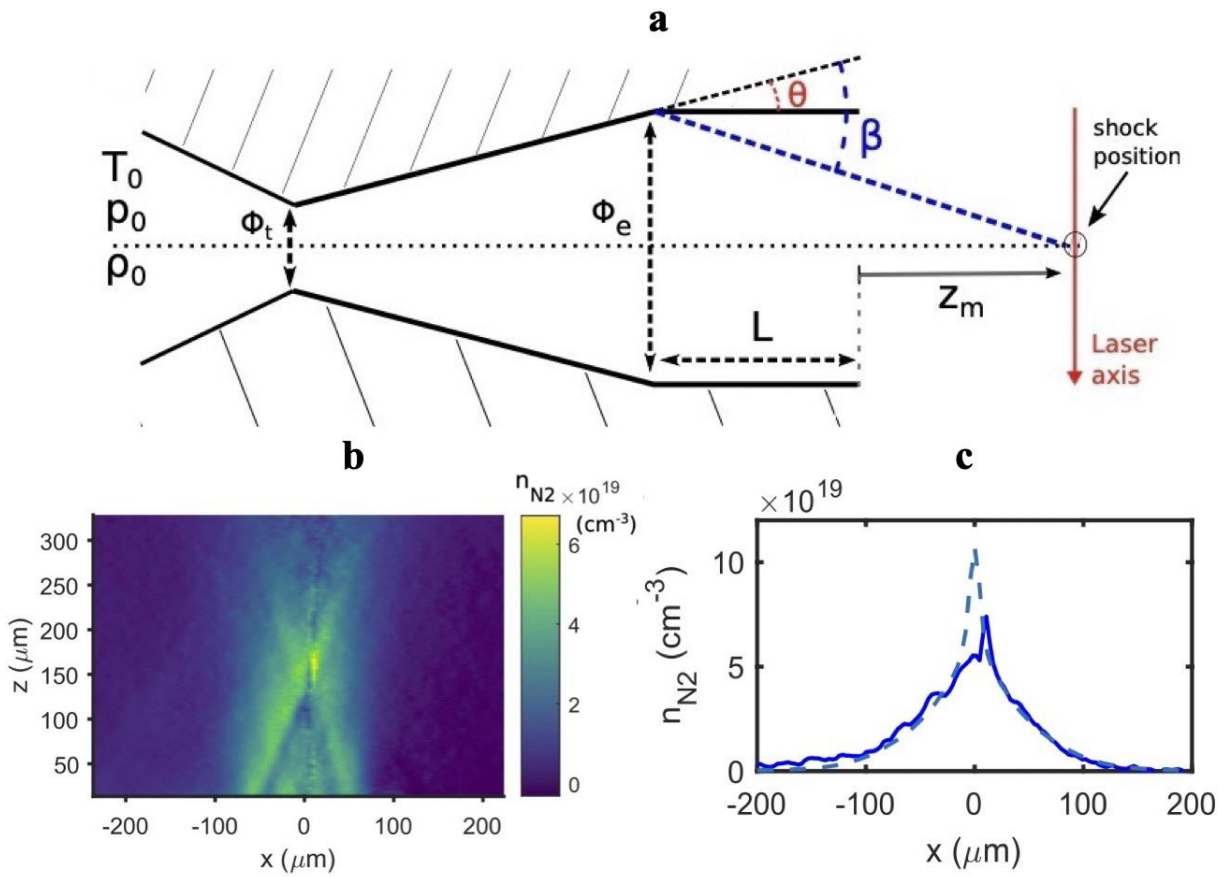

Figure 3: *A diagram of the formation of an oblique shock formation in a symmetrical shock nozzle (a). Experimental nitrogen molecular density map of a symmetric shock nozzle with a backing pressure Pback = 50 bar (b) and comparison of the simulated (dashed) and measured (solid) density profiles at z = zm (c).*

Both profiles have similar widths, but the peak density is significantly lower in the experimental case. This could be due to an insufficient resolution (phase resolution is 3.2 μm) combined with the high on-axis noise of the Abel inversion used to retrieve the density from the measured phase. With a backing pressure P_{back} = 50 bar, the nitrogen density up to 2.8×10^{20} cm^{-3} at z_m = 310 μm is predicted with this design, which corresponds to a plasma density $n = 2.8 \times 10^{21} cm^{-3} = 1.6 n_c$ critical plasma concentration at λ =800 nm after ionisation of N_2 into $N5^+$. Symmetric shock nozzles, therefore, make it possible to reach near-critical to over-critical densities without the need to use a high-pressure compressor.

5. Micrometric One-Side-Shocked nozzles for laser-plasma interaction

A similar method for the formation of the shock-front at one side of a nozzle directly incorporated in the design of the nozzle was implemented. The nozzle has a flat section added at the end of one side of the nozzle. These nozzles are referred to as “One-Sided Shock” (OSS) nozzles. The flat section induces an abrupt change of direction in the gas flow resulting in a shock-front formation and creating a sharp density gradient downstream [2,5]. In Fig. 4a, the picture of an OSS nozzle with a 100 µm throat and 300 µm exit diameter “De Laval” nozzle with a 100 µm long flat section is shown. The nozzle was manufactured from fused silica using the FLICE technique. Due to the asymmetric configuration, 3D computational fluid dynamics (CFD) simulations were conducted using ANSYS Fluent software to validate and optimise the design. Fluid simulations gave the N_2 molecular density, from which the corresponding plasma density by assuming ionisation up to N^{5+} was retrieved. The plasma density profile was characterised experimentally by sending the laser pulse into a nitrogen gas jet produced from the OSS nozzle. The plasma column produced by the main beam was illuminated from the side by a probe beam and imaged on a quadriwave lateral shearing interferometer (SID4-HR, Phasics, [4]). In Fig 4b, the measured plasma concentration obtained using nitrogen gas with a backing pressure of 15 bar is shown.

At the height of 150 µm above the nozzle exit, the measured length of the density downward transition is 16 µm (18 µm in the simulation), and the density drop is 26% (21% in the simulation). At the height of 200 µm, the measured length of the density downward transition is 26 µm (27 µm in the simulation) with a density drop of 31% (24% in the simulation). This new asymmetric design is particularly well suited to small targets, where inserting a knife-edge for the creation of a downward

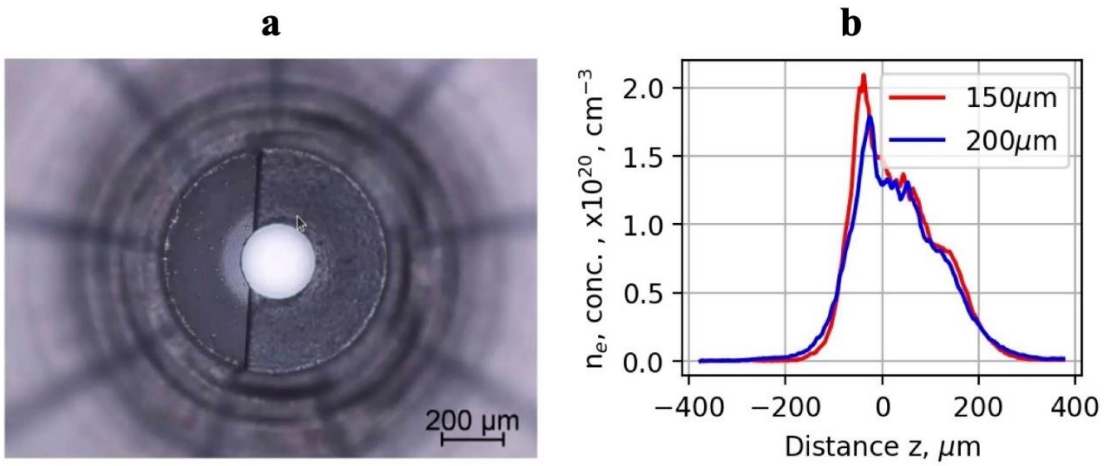

Figure 4: *The top view of a 100/300 µm OSS nozzle (a) and measured plasma concentration dependence on distance from nozzle axis at 150 and 200 µm above the nozzle outlet was obtained using nitrogen gas with a backing pressure of 15 bar (b).*

gradient in the flow can be difficult. A single-piece micronozzle for a shock-formation can benefit in a large number of applications in laser-plasma experiments.

6. High energy Slit nozzles for laser-plasma interaction

In addition to the symmetrical and asymmetrical shocked nozzles, a combined slit nozzle with an electron injector for a 100 TW class laser was developed (Fig. 5a). The shocked nozzles produce sharp micro-scale density gradients, but they are not suited for generating cm-length gas jets. Long and homogeneous centimetre scale plasma targets are required for accelerating electrons to high energies of hundreds of MeV. The precise tailoring of the downward plasma gradient at the 10 µm level is of high importance for controlling the electron injection. In Fig. 5, the view and tomographic slice of a combined slit nozzle with a throat of 0.2x1.4 mm and a centimetre long outlet slit of 0.65x10 mm is shown. The straight section at the beginning of the slit produces the injection of electrons. Due to the relatively large nozzle dimensions, the nozzle was manufactured using the nanosecond rear rear-side processing technique only.

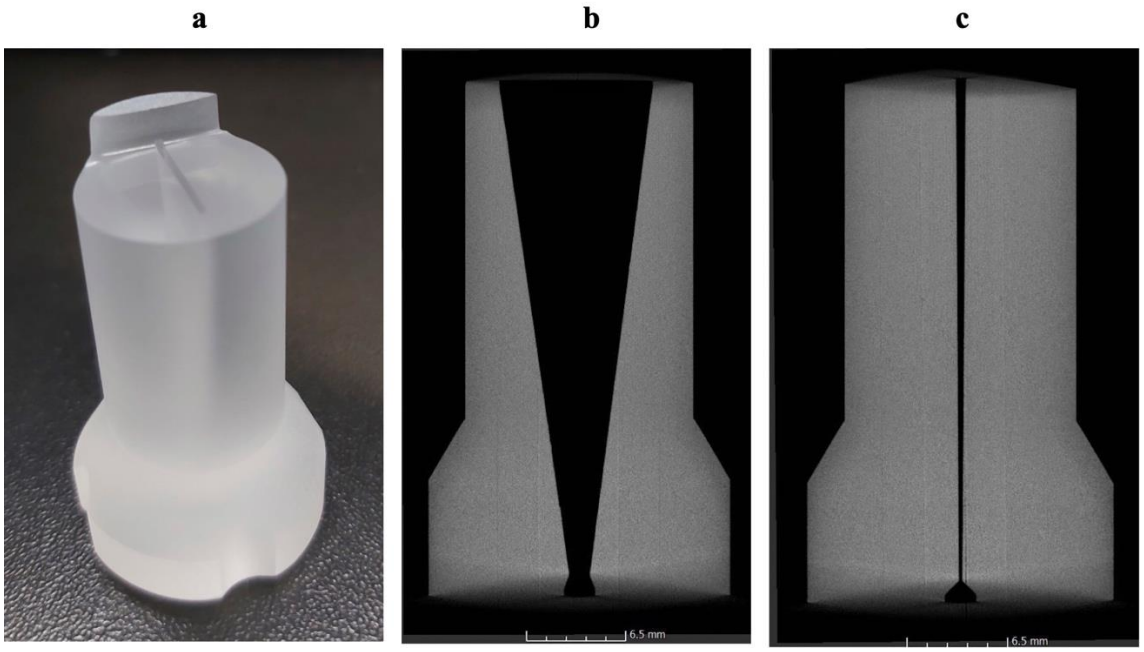

Figure 5: *The view of a combined 1-cm long slit nozzle with a one-side straight section for the producing of a micrometric downward plasma concentration gradient and injection of electrons (a). Tomographic slices of the slit nozzle with a throat of 0.2x1.4 mm and output slit of 0.65x10 mm (b, c).*

In Fig. 6 and Fig. 7, the 3D simulation of plasma density distribution using ANSYS Fluent software is presented. The simulation results show that the One-Side-Shock section produces a 200-300 μm long downramp transition with a ~ 40% drop of gas concentration controlling the injection of electrons. The transition zone is followed by a 1 cm long laser acceleration section with a homogenous plasma distribution. The proposed combined slit nozzle can be implemented to accelerate electrons to the hundreds of MeV and lower the divergence and energy spread of the electron beam because of the better control of the injection of electrons.

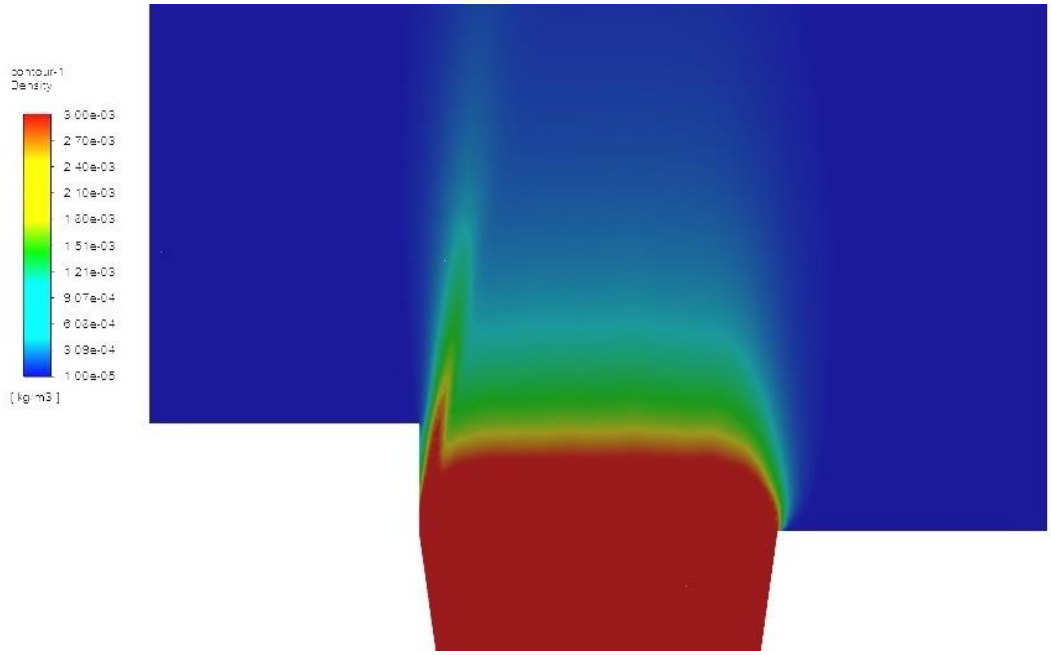

Figure 6: *3D ANSYS Fluent simulation of the plasma density distribution at the backing pressure of p=15 bar.*

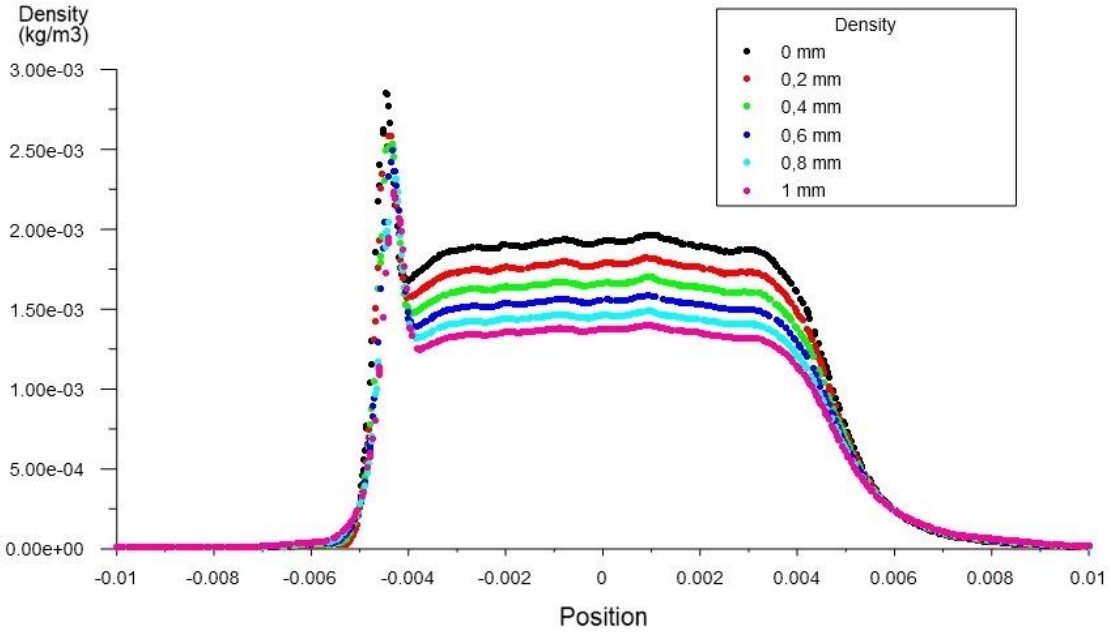

Figure 7: *The simulated dependence of the plasma density on the distance above the nozzle exit at the backing pressure p=15 bar.*

7. Conclusions

In the scope of the work package 6.3, four types of innovative targets for laser-plasma accelerators (LWFA) were simulated, manufactured and characterised. The micrometric supersonic nozzles with the throat diameter down to 40 µm and shocked nozzles can be implemented for laser wakefield acceleration with kHz class 1 TW systems. A combined 1-cm long slit nozzle with an OSS section ensures better parameters of electron beams accelerated by 100 TW lasers. New methods of the injection of electrons and the separation of the injection section and acceleration stage of electrons enable better control of the plasma target properties in the energy range between few and hundreds of MeV.

The hybrid nanosecond rear-side processing and Femtosecond Laser-assisted Selective Chemical Etching technique allows the fabrication of 1 cm long fused silica nozzles with an accuracy of 10 µm. The dielectric nozzles, compared to the metallic ones, have a higher damage threshold and thus better reliability. In future work, the production of double gas jets with different ionisation energy is planned. It will facilitate better control of the amount of injected charge. The manufactured nozzles will be implemented for LWFA of electrons and tested at laser-plasma acceleration facilities of CNRS/LOA. The nozzle design will be verified and optimised based on the experimental results.

8. References

1. V. Tomkus, V. Girdauskas, J. Dudutis, P. Gečys, V. Stankevič, G. Račiukaitis, High-density gas capillary nozzles manufactured by hybrid 3D laser machining technique from fused silica, Opt. Express. 26, 27965, (2018), https://doi.org/10.1364/OE.26.027965
2. L. Rovige, J. Huijts, I. A. Andriyash, A. Vernier, M. Ouillé, Z. Cheng, T. Asai, Y. Fukuda, V. Tomkus, V. Girdauskas, G. Raciukaitis, J. Dudutis, V. Stankevic, P. Gecys, R. Lopez-Martens, and J. Faure, Optimization and stabilization of a kilohertz laser-plasma accelerator, Physics of Plasmas 28, 033105 (2021), https://doi.org/10.1063/5.0040926
3. L. Martelli, Analyse au Micro-Tomographie, Thales Laboratoire d'analyse AVS, France Sas - Vélizy(4164), N° 03281 23/07/2021, N°03434 29/10/2021, N° 03493 17/11/2021.
4. J. Primot and L. Sogno, “Achromatic three-wave (or more) lateral shearing interferometer,” J. Opt. Soc. Am. A 12, 2679–2685 (1995). plasma accelerator, Physics of Plasmas 28, 033105 (2021), https://doi.org/10.1063/5.0040926 .
5. J. L. Rovige, J. Huijts, A. Vernier, I. Andriyash, F. Sylla, V. Tomkus, V. Girdauskas, G. Raciukaitis, J. Dudutis, V. Stankevic, P. Gecys, and J. Faure, Symmetric and asymmetric shocked gas jets for laser-plasma experiments, Rev. of Sci. Instr., 92, 083302 (2021); https://doi.org/10.1063/5.0051173